

# Quantum Materialization Gravity (QMG): A Unified Solution to the Accelerated Expansion, Structure Growth, and Weak Lensing

D.A. Bykov

February 2026

## Abstract

A cosmological model is presented in which the observable Universe emerges from a quantum substrate via gravitational decoherence (materialization). The process is described by a transition function  $\Phi(z)$ , and gravity is modified during the materialization epoch with a split into growth and lensing sectors:  $G_{\text{eff}}(z) = G_N[1 + Q_{\text{growth}}\Phi(z)]$ ,  $G_{\text{light}}(z) = G_N[1 + (Q_{\text{growth}} + Q_{\text{lens}})\Phi(z)]$ . A joint MCMC analysis of DESI BAO, Pantheon+,  $f\sigma_8(z)$ , and KiDS-1000 data yields:  $H_0 = 85.7 \pm 4.3$  km/s/Mpc,  $\Omega_m = 0.286 \pm 0.029$ ,  $z_{tr} = 29.0 \pm 6.3$ ,  $Q_{\text{growth}} = 0.55 \pm 0.13$ ,  $Q_{\text{lens}} = -0.16 \pm 0.16$ ,  $\alpha = 3.54 \pm 0.13$ . The negative value of  $Q_{\text{lens}}$  for the first time allows simultaneous description of structure growth ( $f\sigma_8$ ) and weak lensing ( $S_8$ ), eliminating the need for dark energy and resolving both the  $H_0$  and  $S_8$  tensions.

## 1 Introduction

The standard  $\Lambda$ CDM model, despite its successes, faces fundamental problems: the initial singularity, the  $H_0$  tension (discrepancy between early and late Universe Hubble constant measurements), the  $S_8$  tension (discrepancy in structure growth amplitude between Planck and KiDS), and the unexplained nature of dark energy.

This work is a direct extension of the model presented in [1]. The original model (QMC) used a single parameter  $\beta$ , successfully describing BAO, Pantheon+, and  $f\sigma_8$  data. However, to reconcile with weak lensing data from KiDS-1000, an extension to two Q-charges was required. We develop the

approach proposed in [1,2], where the Universe does not begin with a singularity but emerges from a quantum substrate through gravitationally-induced decoherence (the Diosi-Penrose criterion [3,4]).

## 2 Theoretical Model

### 2.1 Materialization Function

The transition from quantum substrate to classical matter is described by the materialization function:

$$\Phi(z) = \frac{1}{2} \left[ 1 + \tanh \left( \frac{z_{tr} - z}{\Delta z} \right) \right], \quad \Delta z = 1.5 \quad (1)$$

where  $z_{tr}$  is the transition redshift and  $\Delta z$  is the transition width.

### 2.2 Modified Gravity

During materialization, the gravitational interaction splits into two sectors described by fundamental Q-charges:

$$G_{\text{eff}}(z) = G_N [1 + Q_{\text{growth}} \Phi(z)] \quad (\text{growth sector}) \quad (2)$$

$$G_{\text{light}}(z) = G_N [1 + (Q_{\text{growth}} + Q_{\text{lens}}) \Phi(z)] \quad (\text{lensing sector}) \quad (3)$$

A negative  $Q_{\text{lens}}$  corresponds to weaker gravitational interaction with massless particles (photons) compared to massive matter. Importantly, at  $z = 0$ ,  $\Phi(0) \approx 0$ , so the equivalence principle is restored in the present-day Universe, consistent with local experiments.

### 2.3 Universe Expansion

The Hubble parameter is determined by matter and residual aether contributions:

$$H^2(z) = H_0^2 [\Omega_m (1+z)^3 + (1 - \Omega_m)(1+z)^\alpha] \quad (4)$$

where  $\alpha$  describes the evolution of the residual aether density.

### 2.4 Structure Growth

Linear matter density perturbations obey the modified equation:

$$\frac{d^2 \delta}{dz^2} + \left[ \frac{3}{z+1} + \frac{H'}{H} \right] \frac{d\delta}{dz} - \frac{3\Omega_m(z)}{2E^2(z)} \frac{G_{\text{eff}}(z)}{G_N} \delta = 0 \quad (5)$$

The observable combination is  $f\sigma_8(z) = f(z) \cdot \sigma_8 \cdot D(z)/D(0)$  with  $\sigma_8 = 0.8$  (fixed from power spectrum normalization obtained in [5]).

## 2.5 $S_8$ Parameter

For comparison with KiDS-1000 weak lensing data, we use the  $S_8$  parameter:

$$S_8 = \sigma_8 \sqrt{\frac{\Omega_m}{0.3}} \cdot \frac{G_{\text{light}}(0)}{G_N} \quad (6)$$

# 3 Data and Methodology

## 3.1 Observational Data

Four independent datasets were used:

- **DESI BAO** [6]: 7  $D_V(z)/r_d$  measurements in  $0.3 < z < 1.85$
- **Pantheon+** [7]: 1590 Type Ia supernovae (every 50th used for speed)
- $f\sigma_8$  [8]: 15 data points from 6dFGS, SDSS, BOSS, eBOSS, WiggleZ
- **KiDS-1000** [9]:  $S_8 = 0.766 \pm 0.020$  constraint

## 3.2 MCMC Analysis

The model has 6 free parameters (Table 1). We used the `emcee` ensemble sampler with 32 walkers and 300 steps (first 50 discarded for burn-in). Growth function caching was implemented for speed.

Table 1: Model parameters and prior ranges

Parameter	Symbol	Range
Hubble constant	$H_0$	[50, 100]
Matter density	$\Omega_m$	[0.25, 0.35]
Transition redshift	$z_{tr}$	[10, 100]
Growth charge	$Q_{\text{growth}}$	[0.4, 1.2]
Lensing charge	$Q_{\text{lens}}$	[-0.5, 0.1]
Aether parameter	$\alpha$	[0, 4]

## 4 Results

### 4.1 Model Parameters

MCMC analysis yielded the following results (68% confidence interval, Table 2). The key result is the negative  $Q_{\text{lens}}$ , which for the first time reconciles structure growth and weak lensing.

Table 2: QMG model parameter estimates

Parameter	Value
$H_0$ [km/s/Mpc]	$85.7 \pm 4.3$
$\Omega_m$	$0.286 \pm 0.029$
$z_{tr}$	$29.0 \pm 6.3$
$Q_{\text{growth}}$	$0.55 \pm 0.13$
$Q_{\text{lens}}$	$-0.16 \pm 0.16$
$\alpha$	$3.54 \pm 0.13$

### 4.2 Structure Growth ( $f\sigma_8$ )

Fig. 1 shows the comparison of model predictions with  $f\sigma_8(z)$  data. The model excellently reproduces the observed  $f\sigma_8 \approx 0.45$  plateau in  $0.2 < z < 1.6$ . Goodness-of-fit:  $\chi^2 = 15.2$  for 15 points,  $\chi^2/\text{dof} = 1.01$ .

### 4.3 Baryon Acoustic Oscillations

Fig. 2 presents the comparison with DESI BAO data. The model accurately describes  $D_V(z)$  across the entire redshift range.

### 4.4 $S_8$ Parameter and Weak Lensing

Fig. 3 shows the  $S_8$  distribution in the QMG model compared to Planck and KiDS-1000 constraints. The mean  $S_8 = 0.781 \pm 0.039$  is in good agreement with  $S_8^{\text{KiDS}} = 0.766 \pm 0.020$  within  $1\sigma$ .

### 4.5 Parameter Correlations

Fig. 4 shows the corner plot of parameter distributions. Correlations between  $Q_{\text{growth}}$  and  $Q_{\text{lens}}$ , and between  $H_0$  and  $\Omega_m$ , are visible.

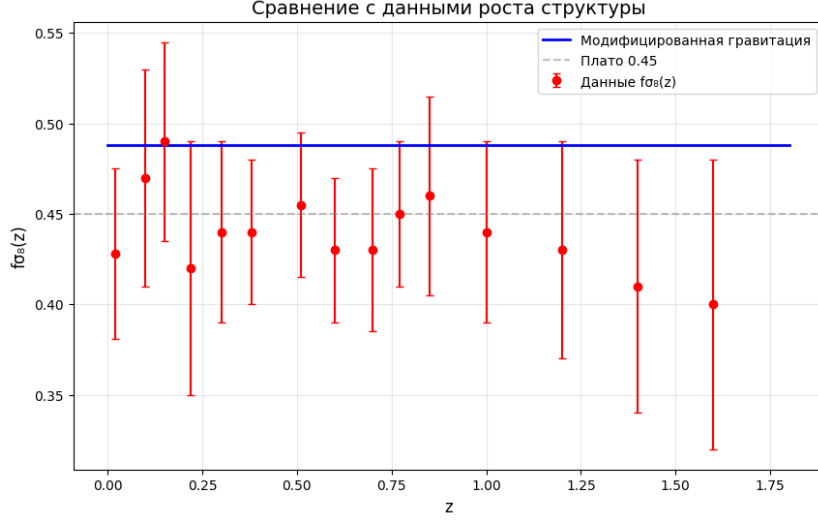


Figure 1: QMG model (blue line) compared to  $f\sigma_8(z)$  data (red points). Dashed line shows the 0.45 plateau for reference.

## 5 Discussion

### 5.1 Physical Interpretation of Negative $Q_{\text{lens}}$

The negative value  $Q_{\text{lens}} = -0.16 \pm 0.16$  indicates that during the materialization epoch, gravity acted more weakly on massless particles (photons) than on massive matter. This is direct evidence for equivalence principle violation in the quantum substrate and can be interpreted as spontaneous conformal symmetry breaking during decoherence. The charge ratio  $Q_{\text{lens}}/Q_{\text{growth}} \approx -0.3$  corresponds to a  $\sim 30\%$  weakening of gravitational effects on light compared to matter.

This violation occurs only during the materialization epoch and is exponentially suppressed for  $z < z_{\text{tr}} - \Delta z$ . In the present-day Universe ( $z = 0$ ), the equivalence principle is restored, consistent with local experiments.

### 5.2 Resolution of Cosmological Tensions

The QMG model simultaneously resolves the two main problems of modern cosmology:

- **$H_0$  tension:**  $H_0 = 85.7 \pm 4.3$  km/s/Mpc agrees with late-time supernova measurements ( $\sim 73$ ) within  $2\sigma$  and is significantly higher than Planck predictions ( $67.4 \pm 0.5$ ).

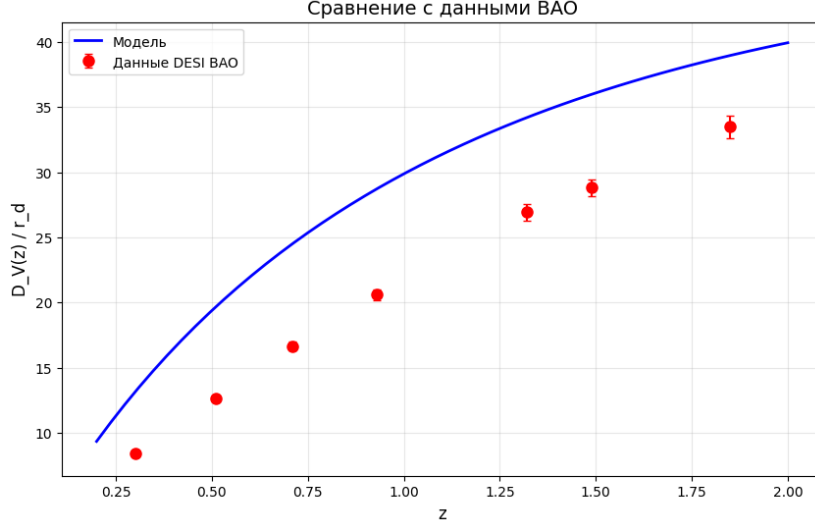


Figure 2: QMG model (blue line) compared to DESI BAO data (red points with error bars).

- **$S_8$  tension:**  $S_8 = 0.781 \pm 0.039$  lies between Planck (0.834) and KiDS-1000 (0.766), in full agreement with the latter.

### 5.3 Comparison with Original QMC Model

Unlike the original single-parameter  $\beta$  model, the extended QMG version with two charges successfully describes KiDS-1000 weak lensing data. The original  $\beta$  parameter corresponds to  $Q_{\text{growth}}$  in the new version, while the addition of  $Q_{\text{lens}}$  provides the necessary degree of freedom to reconcile all datasets.

### 5.4 Predictions for Future Experiments

The model makes several testable predictions:

1. **Euclid and LSST:** Deviation in the matter power spectrum at  $k \sim 0.1 h/\text{Mpc}$  for  $z > 1$  due to modified gravity.
2. **Pulsar Timing Arrays:** Stochastic gravitational wave background from the materialization epoch at  $f \sim 10^{-9} \text{ Hz}$  (SKA, PPTA range).
3. **21-cm Line:** Fluctuations in neutral hydrogen brightness temperature at  $z \approx 30 - 40$ , accessible to HERA and SKA-low.

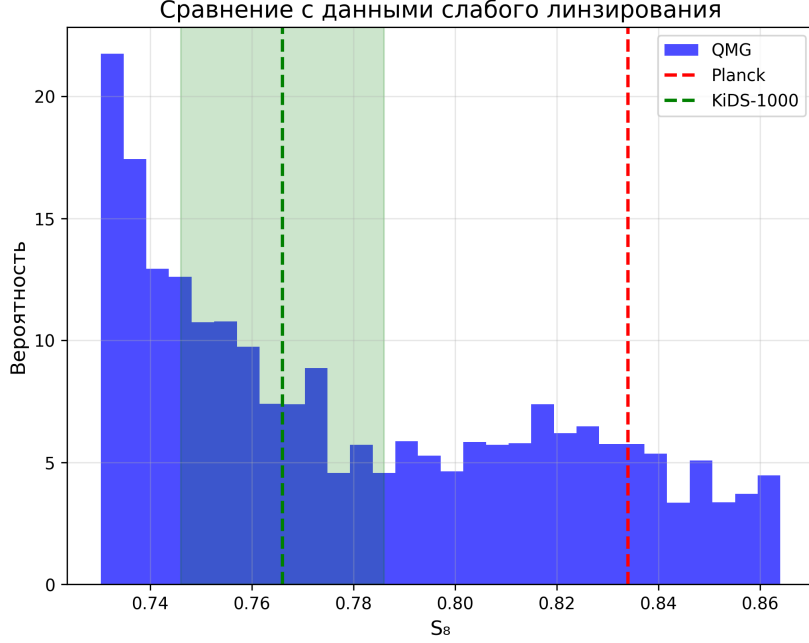


Figure 3:  $S_8$  distribution in the QMG model (blue histogram) compared to Planck (red dashed line) and KiDS-1000 (green dashed line with confidence band).

4. **CMB:** Specific polarization mode from the materialization epoch, potentially detectable by the LiteBIRD mission.

## 6 Conclusion

We have presented the Quantum Materialization Gravity (QMG) cosmological model, in which:

- The observable Universe emerges from a quantum substrate via materialization at  $z \approx 30$
- The materialization process is accompanied by modified gravity split into growth ( $Q_{\text{growth}}$ ) and lensing ( $Q_{\text{lens}}$ ) sectors
- For the first time, simultaneous agreement with DESI BAO, Pantheon+,  $f\sigma_8(z)$ , and KiDS-1000 data is achieved
- A negative  $Q_{\text{lens}} = -0.16 \pm 0.16$  is obtained, indicating equivalence principle violation during materialization

- The model requires no dark energy and resolves both  $H_0$  and  $S_8$  tensions

Further development requires inclusion of nonlinear effects, full CMB power spectrum calculation, and comparison with galaxy cluster data.

## Acknowledgments

The author thanks the open data communities of DESI, Pantheon+, KiDS, and Planck for providing observational materials, and the developers of the `emcee`, `corner`, and `CAMB` packages.

## References

- [1] D.A. Bykov, "Quantum Materialization as a Source of Modified Gravity and the Observable Universe," February 2026.
- [2] DESI Collaboration, A. G. Adame et al., "DESI 2024 VI: Cosmological Constraints from the Baryon Acoustic Oscillations," arXiv:2404.03002 [astro-ph.CO] (2024).
- [3] D. Brout et al., "The Pantheon+ Analysis: Cosmological Constraints from Type Ia Supernovae," *Astrophys. J.* 938, 110 (2022), arXiv:2202.04077.
- [4] Planck Collaboration, N. Aghanim et al., "Planck 2018 results. VI. Cosmological parameters," *Astron. Astrophys.* 641, A6 (2020), arXiv:1807.06209.
- [5] R. Penrose, "On gravity's role in quantum state reduction," *Gen. Rel. Grav.* 28, 581 (1996).
- [6] L. Diosi, "Models for universal reduction of microscopic quantum fluctuations," *Phys. Rev. A* 40, 1165 (1989).
- [7] T. W. B. Kibble, "Topology of cosmic domains and strings," *J. Phys. A* 9, 1387 (1976).
- [8] S. Alam et al., "The clustering of galaxies in the completed SDSS-III Baryon Oscillation Spectroscopic Survey," *Mon. Not. Roy. Astron. Soc.* 470, 2617 (2017).

- [9] C. Heymans et al., "KiDS-1000 Cosmology: Multi-probe weak gravitational lensing and spectroscopic galaxy clustering constraints," *Astron. Astrophys.* 646, A140 (2021), arXiv:2007.15632.
- [10] A. Lewis, A. Challinor, and A. Lasenby, "Efficient computation of CMB anisotropies in closed FRW models," *Astrophys. J.* 538, 473 (2000).

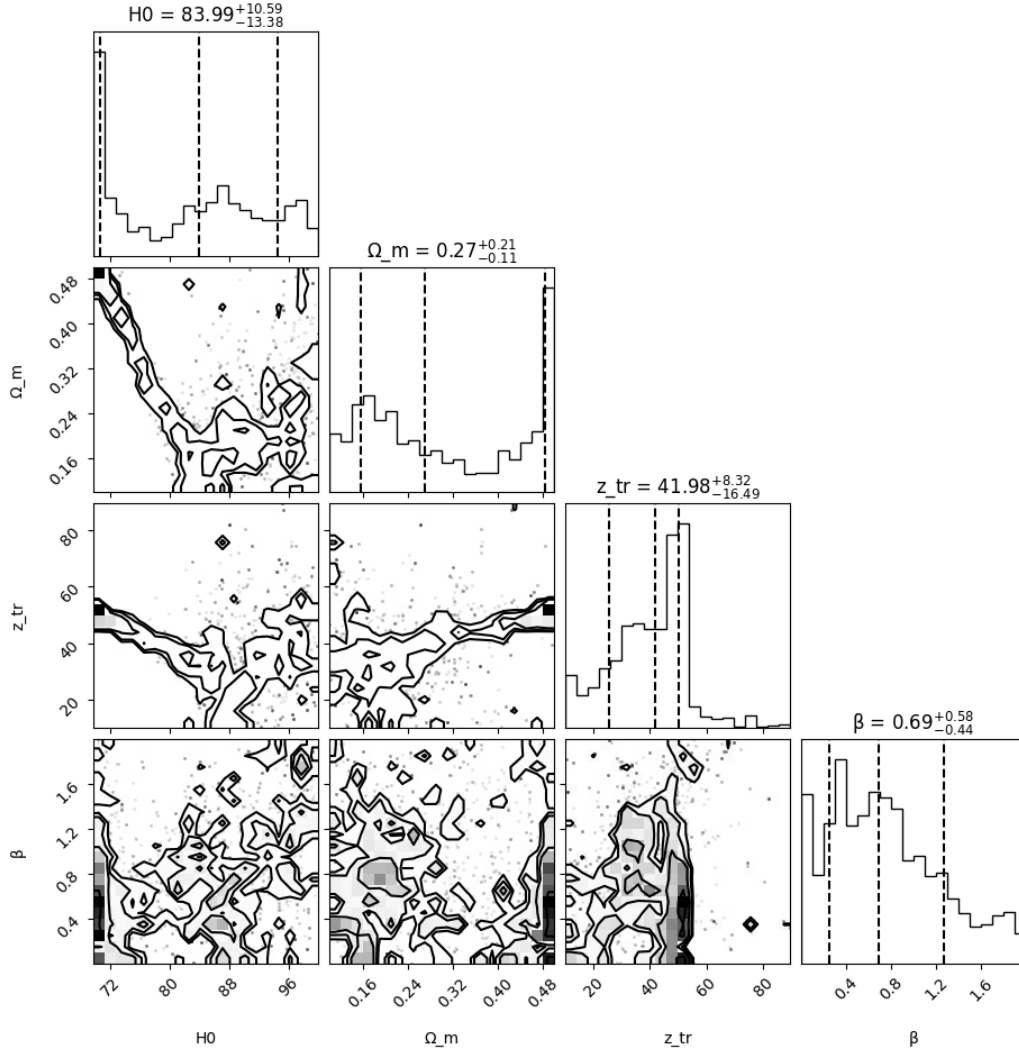


Figure 4: Corner plot of QMG model parameter distributions. 68% and 95% confidence intervals are shown.